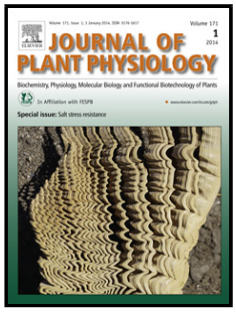

Title: Hormonal and metabolic responses of Mexican lime plants to CTV infection

Authors: Rosa María Pérez-Clemente, Almudena Montoliu, Vicente Vives-Peris, Vicent Arbona, Aurelio Gómez-Cadenas

PII: S0176-1617(19)30058-6
DOI: https://doi.org/10.1016/j.jplph.2019.05.001
Reference: JPLPH 52974

To appear in:

Received date: 20 February 2019
Revised date: 6 May 2019
Accepted date: 7 May 2019

Please cite this article as: Pérez-Clemente RM, Montoliu A, Vives-Peris V, Arbona V, Gómez-Cadenas A, Hormonal and metabolic responses of Mexican lime plants to CTV infection, *Journal of Plant Physiology* (2019), https://doi.org/10.1016/j.jplph.2019.05.001

Hormonal and metabolic responses of Mexican lime plants to CTV infection

Rosa María PÉREZ-CLEMENTE, Almudena MONTOLIU, Vicente VIVES-PERIS, Vicent ARBONA, Aurelio GÓMEZ-CADENAS*

Departament de Ciències Agràries i del Medi Natural, Universitat Jaume I, Avda. Sos Baynat s/n, 12071, Castellón de la Plana, Spain

*Corresponding author: Aurelio Gómez-Cadenas Departament de Ciències Agràries i del Medi Natural, Universitat Jaume I, Avda. Sos Baynat s/n, 12071, Castellón de la Plana, Spain Phone: +34 964 729402

e-mail: aurelio.gomez@uji.es

ABSTRACT

Plant viral infections alter gene expression and metabolism in infected host. To study the molecular responses of Mexican lime to CTV infection, an analysis of plant metabolome in response to infection with severe (T318) or mild (T385) isolates of CTV was performed. Healthy plants and those infected with any of the two virus strains showed different metabolite profiles, at different stages of new sprout development. Proline content increased in plants infected with CTV, proportionally to the virulence of the virus strain. Abscisic acid content decreased after virus infection whereas jasmonic and salicylic acid levels increased. CTV infection had an impact on plant secondary metabolism, by stimulating the synthesis of different metabolites such as L-

methylhistidine, phenylpropanoid derivatives. These metabolites are common responses of different organisms, including higher mammals, to viral diseases, and its presence in this system points to the existence of universal responses to virus infection among different kingdoms.

Keywords

Citrus aurantifolia; CTV; Metabolome; Abscisic acid; Salicylic acid; Jasmonic acid

Abbreviations

ABA, abscisic acid; APX, ascorbate peroxidase; CTV, *Citrus tristeza virus*; Et, ethylene; ESI-QqTOF-MS, high-resolution quadrupole time-of-flight mass spectrometry along with an electrospray ionization source; GC, gas chromatography; GPX, glutathione peroxidase; GR, glutathione reductase; HPLC, high performance liquid chromatography; JA, jasmonic; LC, liquid chromatography; MS, mass spectrometry; PLS-DA, Discriminant Analysis of Partial Least Squares; QTOF, hybrid quadrupole time-of-flight mass spectrometers; SA, salicylic acid; SOD, superoxide dismutase; TMV, *Tobacco mosaic virus*;

1. Introduction

Viruses induce varied physiological, metabolic and developmental changes in infected plants. Symptoms of viral infections are the result of alterations in plant growth and development, as a consequence of the interactions of specific virus factors with cell components, and alterations in hormone synthesis and signaling pathways (Culver and Padmanabhan, 2007).

Interactions of different plant-biotic stressor have shown that plant responses are controlled by hormone-regulated pathways, including salicylic acid (SA), jasmonic acid (JA) and ethylene (Et) (Santner et al., 2009). Abscisic acid (ABA), a key hormone

controlling plant responses to abiotic stress (Arbona and Gómez-Cadenas, 2008; Gómez-Cadenas et al., 2015), seems to have different roles in plant pathogen defense depending on the time after infection. During the early stages after infection, ABA induces stomatal closure and callose deposition and at later stages suppresses reactive oxygen species accumulation and SA induction (Ton et al., 2009).

Newly developed techniques have allowed evaluating the impact of different stress conditions at the whole metabolic level on sensitive and tolerant plant species (Arbona et al., 2010; Argamasilla et al., 2013). Metabolite profiling allows a comprehensive evaluation of the metabolome, the pool of low molecular weight molecules in a given plant tissue in a specific developmental stage and under specific environmental conditions. Mass spectrometry (MS) coupled to separative techniques such as liquid chromatography (LC), gas chromatography (GC), or capillary electrophoresis is used for this purpose (Argamasilla et al., 2013). Indeed, LC coupled to hybrid quadrupole time-of-flight mass spectrometers (QTOF) are among the most versatile metabolite profiling techniques because LC is the most compatible technique with biomolecules, and the accurate mass measurement, true isotopic pattern recognition, and a high sensitivity provided by QTOF instruments are suitable for calculations on elemental composition of mass signals (Glauser et al., 2013).

Citrus tristeza virus (CTV) is one of the most devastating plant viruses worldwide. Different CTV epidemics have been responsible for the death of more than 100 million citrus trees propagated on *Citrus aurantium* L. rootstock, and more recently, many millions more, propagated on decline-tolerant rootstocks, are weakened by severe CTV isolates inducing stem pitting in commercial citrus varieties regardless of the rootstock used (Moreno and Garnsey 2010).

Among citrus genotypes, Mexican lime (*C. aurantifolia* [Christm.] Swing) is known to be the most sensitive citrus species to Tristeza virus and, in fact, diagnosis of CTV infection has been performed for years by biological indexing on this sensitive host (Moreno et al., 1993).

It has been recently reported that CTV causes the impairment of the photosynthetic machinery in the infected plants. As a consequence of the impairment in the photosynthetic system, infected leaf cells suffer oxidative damage. Despite that Mexican lime infected plants exhibit some ability for H_2O_2 detoxification by activating antioxidant enzyme activities (ascorbate peroxidase, APX; superoxide dismutase, SOD; or glutathione peroxidase, GPX), these defense mechanisms are insufficient to overcome the stress imposed by the virus infection (Dória et al., 2015; Pérez-Clemente et al., 2015).

Although it is well-known that virus infection results in the alteration of biochemical processes within the plant; there is a lack of information on the metabolic changes associated to this response, apart from the primary metabolism and volatile organic compounds of their host (Killiny et al., 2017).

In the present work, we have studied the hormonal and metabolic responses of Mexican lime plants subjected to stress caused by CTV infection. Endogenous ABA, JA, and proline contents were measured as important physiological responses in plants infected with either severe (T318) or mild (T385) CTV strains. In addition, changes in secondary metabolite profiling due to CTV infection were analyzed.

2. Materials and methods

2.1. Plant material, virus strains and plant inoculation

Experiments were performed using Mexican lime (*Citrus aurantifolia* (Christm.) Swing.) plants. This genotype is highly susceptible to infection by CTV. The strains T318 and T385 used in this study are part of a collection kept at the Instituto Valenciano de Investigaciones Agrarias (Moncada, Spain) and were kindly provided by Dr. Pedro Moreno. T385 is a mild strain that only induces inconspicuous vein clearing in Mexican lime, whereas T318 is a severe strain inducing strong vein clearing and stem pitting in lime and other citrus species (Moreno et al., 1993). These strains are maintained in container-grown sweet orange plants propagated on Carrizo citrange (*C. sinensis* L. Osb. x *Poncirus trifoliata* L. Raf.) rootstock in an insect-proof greenhouse.

For this study, Mexican lime seedlings were graft-inoculated with two bark pieces from plants infected with either CTV strain or from healthy plants (6 plants per treatment). Limes were grown in a greenhouse (18/26 ºC night/day) and 60-85% relative humidity using an artificial potting mix (50% sand and 50% peat moss). During this period, plants were watered three times a week with a half-strength Hoagland solution (Argamasilla et al., 2013). CTV infection was confirmed by ELISA with monoclonal antibodies 3DF1 and 3CA5 (Cambra et al., 2000). Plants were kept under the described culture conditions for two years.

For analytical studies, young sprouts with leaves at different developmental stages were collected during the active growing period and immediately frozen in liquid nitrogen. Control and infected plant materials on every developmental stage were separately processed.

2.2. Proline content determination

Proline content was analyzed following the procedure described in (Arbona et al., 2010) Briefly, 0.05 g of frozen plant tissue was homogenized in 5% sulphosalicylic acid (Panreac) using a tissue homogenizer (Ultra-Turrax,). After extraction, homogenates were centrifuged to pellet cell debris at 4ºC and 1 mL aliquot of the supernatant was combined with an equal volume of glacial acetic acid (Panreac) and ninhydrin reagent. This mixture was boiled in a water bath for 1 h and then cooled in an ice bath. The solution was partitioned against 2 mL of toluene (ACS grade; Panreac) and absorbance at 520 nm measured in this organic layer. A calibration curve was performed using commercial proline as standard (Sigma-Aldrich).

2.3. Hormone content determination.

Plant hormones were analyzed by HPLC coupled to tandem mass spectrometry as described in Arbona and Gómez-Cadenas (2008). Briefly, frozen citrus sprouts were ground to a fine powder with a prechilled mortar and a pestle, and then 0.5 g of powdered tissue was extracted in ultrapure water using a tissue homogenizer (Ultra-Turrax). Before extraction, samples were spiked with 100 ng of [$^2H_6$]-ABA, 100 ng of [$^2H_4$]-SA, and 100 ng of dihydrojasmonic acid to assess recovery and matrix loses. After extraction and centrifugation, the pH of the supernatant was adjusted to 3.0 and partitioned twice against diethyl ether (Panreac). The organic layers were combined and evaporated in a centrifuge vacuum evaporator (Jouan). The dry residue was thereafter resuspended in a water:methanol (9:1) solution, filtered, and injected into an HPLC system (Alliance 2695, Waters Corp). Hormones were then separated in a reversed-phase Kromasil 100 C18 column (100 × 2.1 mm 5-µm particle size) using methanol and ultrapure water both supplemented with glacial acetic acid to a concentration of 0.05%. The mass

spectrometer, a triple quadrupole (Quattro LC, Micromass Ltd.), was operated in negative ionization electrospray mode and plant hormones were detected according to their specific transitions using a multiresidue mass spectrometric method (Arbona and Gómez-Cadenas, 2008).

2.4. Sample extraction for metabolite profiling analyses

Frozen plant tissue powder (100 mg) was extracted by sonication (10 min at room temperature) in 350 µl of 80% MeOH (HPLC grade, Panreac) spiked with biochanin A (Sigma-Aldrich, internal standard) at 1 mg/L concentration. After extraction, samples were centrifuged at 10,000 rpm and 4ºC. Thereafter, supernatants were recovered and filtered through PTFE membrane syringe filters directly to amber glass chromatographic vials. All samples were extracted and injected fresh.

2.5. Chromatographic and QTOF-MS conditions

Plant extracts were separated by reversed phase HPLC using acetonitrile (B) and water (A), both supplemented with formic acid to a concentration of 0.1% (v/v), as solvents and a C18 column (5-µm particle size, 100×2.1 mm, XTerraTM, Waters). The separation module, a Waters Alliance 2965 was operated in gradient mode at a flow rate of 300 µl min^{-1} for 30 min as follows: 0-2 min 95:5 (A:B) followed by an increase in B from 5 to 95 in the following 26 min (2.01-28.00 min), thereafter returning to initial conditions (29.01-30.00 min) that were maintained for 5 min for column reconditioning. Column eluates were introduced into a QTOF-MS (Micromass Ltd.) through an ESI source operated in positive and negative mode. Nitrogen was used as the nebulization as well as

the desolvation gas and working flows were set at 100 and 800 L h^{-1}, respectively. Source block temperature was kept at 120ºC and desolvation gas at 350ºC. Capillary, cone, and extractor voltages were set at 4 kV, 25 eV, and 3 eV, respectively. Before analyses, the QTOF-MS was calibrated by infusing a mixture of NaOH and HCOOH at a flow rate of 25 µl min^{-1}. During acquisition, a one-ppm solution of Leu-enkephalin ($[M+H]^+$ 556.2771) was continuously post column infused as a lockmass reference. Data were acquired in positive electrospray ionization and continuous mode in the 50–1000 amu range, scan duration was set at 1.0 s, and interscan delay was set at 0.1 s (Arbona et al., 2010).

2.6. Data Processing

Data processing was achieved using Masslynx v.4.1 and raw data files were analyzed using xcms following conversion to netCDF with the databridge software provided by Masslynx. Chromatographic peak detection was performed using the matchedFilter algorithm, applying the following parameter settings: snr=3, fwhm=15 s, step=0.01 D, mzdiff=0.1 Da, and profmethod=bin. Retention time correction was achieved in three iterations applying the parameter settings minfrac=1, bw=30 s, mzwid=0.05 Da, span=1, and missing=extra=1 for the first iteration; minfrac=1, bw=10 s, mzwid=0.05 Da, span=0.6, and missing=extra=0 for the second iteration; and minfrac=1, bw=5 s, mzwid=0.05 Da, span=0.5, and missing=extra=0 for the third iteration. After final peak grouping (minfrac=1, bw=5 s) and filling in of missing features using the fillPeaks command of the xcms package, a data matrix consisting of mass features (including accurate mass values and retention time) and peak area values per sample was obtained (Argamasilla et al., 2013).

2.7. Metabolite identification

Mass chromatographic features were grouped according to their retention time and annotated as pseudomolecular ions, fragments or adducts. At this step, metabolite database search was performed against Metlin (http://metlin.scripps.edu/index.php), Massbank (http://www.massbank.jp/) and Metfusion (http://msbi.ipb-halle.de/MetFusion/). Potential identities were checked against the experimental fragmentation spectra. When no plausible identification was found, pseudomolecular ions or the most representative ion in each group was labeled as unknown. (Arbona et al., 2010).

2.8. Statistical analyses

Data mean comparisons and regression analyses were performed with STATGRAPHICS PLUS v.5.1. (Statistical Graphics Corporation) software. One-way ANOVA and comparisons between means were made following the LSD test at $P \leq 0.05$. Discriminant Analysis of Partial Least Squares (PLS-DA) was carried out with Simca P+ 11.0, Umetrix AB).

3. Results

3.1. Proline content

Developmental stages were categorized according to leaf number of new sprouts (associated to sprout age): 3-5, 6-8, 9-11 and 12-14 leaves. The pattern of proline

accumulation in the sprouts developed in Mexican lime plants during the first and second year after CTV infection is shown in Figure 1. During the first year, the infection with the severe virus strain induced a significant accumulation of the osmolyte in the new sprouts at different developmental stages. On the contrary, after infection with the mild virus strain, only the most developed sprouts exhibited increased proline levels (Fig. 1a).

Proline concentration in the sprouts developed during the second year after virus infection was significantly higher than in those on non-infected plants regardless the severity of the virus strain, reaching values ranging from 1.50 to 4.05 times higher than controls, Fig. 1b).

3.2. Hormonal *response to CTV infection*

To gain knowledge on the hormonal response of Mexican lime plants to CTV infection, endogenous concentrations of ABA, SA and JA in sprouts developed during the first or second year after infection were determined.

Virus infection induced a reduction in ABA concentration in all stages of sprout development (Fig. 2). The decrease was more drastic in sprouts developed during the second year regardless the severity of the virus strain and the stage of sprout development. In this year there were no statistically significant differences in ABA content between plants inoculated with the mild or the severe virus strains at any stage of sprout development. The greatest differences in ABA content were recorded in sprouts with 12-14 leaves inoculated with the mild strain exhibiting 85.53% reduction compared to controls (Fig. 2b).

On the contrary, the endogenous contents of SA and JA increased as a result of infection. At the first year after infection, highest values for SA content were recorded in the

youngest sprouts (3-5 leaves) infected with the mild strain, being 2.97 higher than in controls and 2.09 times higher than controls in sprouts infected with the severe strain. This pattern of accumulation was maintained throughout the experimental period and in all stages of development (Fig. 3). Similar results were recorded for JA content. In most stages of sprout development, plants infected with the moderate CTV strain exhibited values of this hormone (Fig. 4) higher than control plants or plants infected with the severe CTV strain.

3.3. Metabolite profiling analyses

Analysis of secondary metabolite composition was carried out by means of LC/ESI-QqTOF-MS on extracts from shoots at different growth stages after inoculation with the severe and mild CTV strains. Secondary metabolite profiles were specific of each developmental stage although a number of differences could be observed between control and inoculated plant material and between the two CTV strains (Fig. 5). Significantly altered mass chromatographic features ($p \leq 0.05$ after ANOVA) were grouped according to their relative accumulation in the treatment groups (Supp. Info. 1 and Fig. 5). In general, there were fewer mass signals differentially altered by infection in younger sprouts (3-5 and 6-8 leaves) than in older ones (9-11), but not in the oldest sprouts. In younger sprouts (3-5 and 6-8 leaves), relative levels of most altered chromatographic mass signals increased respect to controls in plants infected with the severe virus strain whereas they decreased in plants inoculated with the mild strain. Nevertheless, in 9-11 leaf-sprouts, the number of mass chromatographic features which intensity was reduced by CTV inoculation increased and then stabilized with age (12-14 leaf-sprouts) (Fig. 6).

3.4 Specific responses to CTV in each developmental stage

In the youngest sprout stage (3 - 5 leaves), compounds annotated as alkaloids increased their concentration in plants inoculated with the severe strain whereas their levels decreased in those inoculated with the mild strain. Flavonoid levels were also enriched in response to CTV infection at this developmental stage. Among flavonoids, anthocyanindin and quercetin derivatives were putatively identified. In general, these compounds were depleted upon infection with CTV, irrespective of the strain employed (Fig. 7).

Lipids are another compound class enriched in this sample group among which membrane phospholipids, fatty acids, oxylipins and limonoids were putatively identified. Conversely to flavonoids, levels of most of these compounds increased in response to CTV infection in a way proportional to the relative virulence of the strain (e.g. heptanoyl choline increased 3.4- and 3.8-fold and unsaturated 18:3 PA 1.5 and 1.6-fold in mild and severe CTV strain-infected leaves, respectively). The triterpenoid obacunone concentration also increased in response to CTV infection (1.8 and 2.2 times respect to control values in plants infected with the mild and the severe strains, respectively). Deacetyl nomilin doubled its concentration in response to the moderate strain (Fig. 7). An oxylipin, 9-hydroxyoctadecatrienoate (9-HOTE), increased also in parallel to the severity of the strain at this developmental stage. Finally, the other compound category enriched at this developmental stage is phenylpropanoids, that mainly decreased upon infection with the moderate strain showing values 50%, 60% and 30% lower than controls (see the glycosylated coumarin, scopolin or 9-hydroxy-4-dimethyloctadienyloxy psoralen). Only caffeoylputrescine increased in response to infection with CTV, with a higher accumulation in plants infected with the severe strain.

In the 6 to 8 leaf stage, the number of annotated compounds was lower (Fig. 8) although the number of total differential mass chromatographic features was higher (Fig. 6). In this group, the identified compounds were mainly depressed by the infection, irrespective of the strain severity. The only exception was the lipids category, in which annotated compounds (germacrene A, linoleic acid and a putative unsaturated phosphatidyl serine) increased greatly in response to the infection with the mild strain showing values between 25.0 and 54.0-fold respect to control values, and the severe strain inducing less pronounced increases (between 3.0 and 11.0 fold). Among phenylpropanoids, a compound annotated as feruloyl glycine isomer 1 was accumulated in Mexican lime tissues following a similar pattern.

In the 9 to 11 leaf stage, most significantly-altered signals decreased their levels in response to the infection. Among flavonoids, only levels of isorhamnetin rutinoside were found to increase in response to infection, showing 4.2- and 4.0-fold change after infection with the moderate and severe strain, respectively, whereas hesperetin concentration only showed a significant increase upon infection with the severe strain whereas inoculation with the mild strain reduced its levels (Fig. 9). Among lipids, levels of three annotated compounds (obacunone, jasmonoyl isoleucine and a putatively annotated farnesylated cysteine) were found to increase in response to infection while the rest showed significant downregulation. In addition, levels of most phenylpropanoids increased in response to infection including *p*-coumaroylputrescine, feruloylputrescine, *p*-coumaroyl-D-glucose, caffeic acid 3-*O*-glucuronide, dihydroferulic acid 4-*O*-glucuronide, isoferulic acid 3-*O*-glucuronide and ferulic acid glucoside. In the 12 to 14 leaf stage, only a few compounds could be putatively annotated including 12-oxophytodienoic acid and feruloylputrescine that showed increased values upon infection with the severe strain (Fig. 10).

4. Discussion

It has been reported that the lack of effective mechanisms for energy dissipation, consequence of CTV infection, may cause more electrons to divert to photorespiration (and/or to the Mehler reaction) instead of being used in photosynthetic processes. Which is in concordance with recent transcriptomic studies performed with *Citrus sinensis*, revealing a strong repression of genes associated to photosynthesis and carbon and nucleic acid metabolism (Fu et al., 2017). This causes an increase in reactive oxygen species such as hydroxyl, singlet oxygen and superoxide anions, and therefore results in higher oxidative damage (Pérez-Clemente et al., 2015). Stress-inducible proline accumulation might act as a component of an antioxidant defense system to counteract the deleterious effects of oxidative stress, by directly scavenging free radicals or by activating antioxidant systems (reviewed in Ben Rejeb et al., 2014). In transgenic citrus plants carrying heterologous pyrroline-5-carboxylate synthetase gene (*P5CS112A*), high endogenous proline content caused an increase in transcript levels of cytosolic APX and chloroplast glutathione reductase (GR) and Cu/Zn SOD isoforms (de Carvalho et al., 2013). Similarly, CTV infection induced an increase in APX activity (Pérez-Clemente et al., 2015), and the expression of genes related with other antioxidant enzymes, GPX and SOD (Dória et al., 2015; Fu et al. 2017). Gandía et al. (2007) reported the overexpression of stress-related genes in lime plants inoculated with the severe CTV isolate T305 whereas infection with T385 induced no significant change. In the present work, it was observed that proline content increased in Mexican lime plants infected with CTV as it has been described in citrus plants cultured under abiotic stress conditions (Arbona and Gómez-Cadenas, 2008; Zandalinas et al., 2016; Vives-Peris et al,. 2017). Proline accumulation in plants infected with the severe strain was higher than in plants infected

with the mild one, indicating that the more intense is the stress, the higher is the proline accumulation (Claussen, 2005). This response has already been observed in other plant species infected with virus, as occurs with *Cucurbita pepo* plants infected with zucchini yellow mosaic virus (Radwan et al., 2007).

Plant hormones play important roles in diverse growth and developmental processes and in various biotic and abiotic stress responses in plants. Infection of plants with diverse pathogens results in changes in levels of various phytohormones (Alazem and Lin, 2015). It has been reported that, to display an effective defense response, plants activate particular signaling pathways that are most likely to enhance resistance to a class of invader (Bigeard et al., 2015). Simultaneously, other signaling pathways with minimal or no significant effects on the invading pathogen may be suppressed to avoid depletion of valuable physiological resources. In this context, it is known that ABA may antagonize many hormone pathways, including SA (Yasuda et al., 2008) and Ethylene/JA pathway (Broekaert et al., 2006). In response to pathogen attack, the acquired systemic response through the SA pathway is activated (Vlot et al., 2009). Our results could reinforce this previously described antagonism and, in fact, data presented here show that the ABA content in infected plants was lower than in control plants throughout the experiment, regardless the virulence of the virus strain used for the infection (Fig. 2).

Although ABA signaling under bacterial or fungal pathogens has been thoroughly studied, ABA profiles under virus infection have been so far poorly addressed. It has been reported that Tobacco Mosaic Virus (TMV) infection increased ABA levels in *Nicotiana tabacum* and tomato. On the contrary, ABA levels did not vary in response to white clover mosaic virus infection in *Phaseolus vulgaris* or in potato cultivars infected with potato virus Y (Alazem and Lin, 2015). Anywise, ABA can have different roles depending on plant susceptibility to a specific virus strain, being accumulated in tolerant lines and not

in susceptible ones (reviewed in Alazem and Lin, 2015). Consequently, the decrease in ABA levels observed in this work could be related to the high sensitivity of Mexican lime plants to the virus. To our knowledge, this is the first work that reports a decreasing pattern of ABA accumulation in woody plants after virus infection. Similar results were previously observed in tissues of citrus plants under abiotic stress conditions, including roots of citrus plants subjected to flooding (Arbona and Gómez-Cadenas, 2008) and shoots and roots of plants subjected to heat stress (Zandalinas et al., 2016), where sensitive rootstocks also decrease ABA content in a higher extent than tolerant ones (Vives-Peris et al., 2017).

Conversely, an accumulation of SA in leaf tissue in response to CTV infection was observed (Fig. 3). This is in agreement with the results described in Zhu et al. (2014), indicating that SA, and its derivative methyl salicylate, serve as a long-distance phloem-mobile systemic resistance signal in several species (tobacco, Arabidopsis, and potato), and are essential for systemic resistance against TMV.

Another example of antagonistic interaction occurs between the SA and the JA signaling pathways in Arabidopsis (Spoel et al., 2003). However, antagonism between the SA and JA signaling pathways does not occur in all cases, and some defense response genes require intact JA, ethylene, and SA signaling pathways after pathogen challenge (Spoel et al., 2003). In the present study, concomitant accumulations of JA and SA were observed in plants infected with CTV virus throughout the experimental period (Fig. 4). These findings may justify an active plant response to the pathogen and suggest that JA could have a role as a mediator between the stress perception and the stimulation of physiological responses, which agrees with previous works (Anderson et al., 2004).

Although it is known that virus infection results in the alteration of physiological, biochemical and metabolic processes within the plant, few metabolomic reports on

plant/virus interactions can be found in the literature. In fact, a complete analysis of metabolites has been only carried out in the case of the hypersensitive response of tobacco plants to TMV (López-Gresa et al., 2012). In the case of CTV infection in citrus plants, only few works with analyses of the primary metabolism and volatile compounds (Killiny et al., 2017) have been performed. Therefore, as indicated, there is a lack of information on how CTV infection affects secondary metabolism in citrus plants. Results derived from metabolite profiling analyses showed that until the 9-11 leaf stage, the number of altered mass signals increased, however, at the 12-14 leaf stage this number was much lower, probably consequence of the infection progression. This could indicate that the ability to modify the secondary metabolism increases simultaneously with sprout development and it can be linked to the higher viral-particles concentration in the most developed sprouts.

Synthesis of secondary metabolites in plants have been proposed to overcome stressful, both, biotic or abiotic, conditions. Among them alkaloids, due to their toxic properties has been suggested as protecting molecules against pathogens. Indeed, several studies report an antioxidant activity for these compounds (reviewed in Matsuura et al., 2014). Results described in this work indicate that alkaloid synthesis was upregulated in the youngest sprouts of plants inoculated with the severe virus strain, and downregulated in the case of those inoculated with the mild strain. This can be a consequence of the attempt of the plant to cope with the more severe oxidative stress detected in young sprouts infected with the severe strain (Pérez-Clemente et al., 2015).

Another metabolite which synthesis was increased in plants inoculated with both kind of virus strains was tentatively annotated as L-methylhistidine ($_{exp}[M+K]^+$ 208.0460, $_{th}[M+K]^+$ 208.0488, ΔmDa 2.8). Although there is no information about its accumulation in plant tissues, this compound has been found to be abnormally accumulated in humans

and other mammals in response to several viral-diseases (see http://www.hmdb.ca/metabolites/HMDB00001; Munshi et al., 2011).

In more developed sprouts (9 to 11 leaf-stage) a repression of the secondary metabolism occurred as a consequence of CTV infection. However, isorhamnetin rutinoside accumulation increased proportionally to the severity of the virus strain. Recently, this metabolite has been isolated in dwarf elder (*Sambucus ebulus* L.), a medicinal plant used for its antioxidant and anti-herpes simplex activities (Zahmanov et al., 2015). As it could be expected, levels of most phenylpropanoids, which are associated with pathogen defense (Hanssen et al., 2011) increased in Mexican lime plants in response to virus infection. In the present study, we showed that the accumulation of the phenylpropanoids *p*-coumaroylputrescine, feruloylputrescine, *p*-coumaroyl-D-glucose, caffeic acid 3-*O*-glucuronide, dihydroferulic acid 4-*O*-glucuronide, isoferulic acid 3-*O*-glucuronide and ferulic acid glucoside was induced in new formed sprouts at 9 to 11 leaves stage. This accumulation of phenylpropanoids is in concordance with the induction of genes related with its biosynthesis pathway observed in previous works with CTV-infected citrus plants (Cheng et al., 2016).

As mentioned above, most phenylpropanoids annotated in this work are coumarins such as scopolin or substituted psoralens, conjugated polyamines such as caffeoylputrescine or glycosylated phenolic acids, known for their role as defensive compounds against biotic (Baumert et al., 2001; Demkura et al., 2012) or abiotic (Argamasilla et al., 2013) threats. In Argamasilla et al. (2013), the accumulation of a ferulic acid derivative and a metabolite annotated as hydroxycinnamyl alcohol was associated to the induction of cell wall synthesis; in the present work, only a metabolite, 5-hydroxyconiferyl alcohol, directly involved in cell wall synthesis was observed in 6-8 leaves sprouts. However, its levels decreased in response to CTV infection, providing no evidence of cell wall growth under

these conditions. Moreover, the phenylpropanoid pathway has been reported as the main route in salicylic acid biosynthesis in leaves of tobacco and potato plants infected with tobacco mosaic virus and potato virus Y, respectively, what remarks the importance of these metabolites in order to improve plant responses against viruses (Kogovšek et al., 2015).

These results point out that some of the metabolites which accumulation occurred in citrus plants after CTV infection are either accumulated in animal tissues in response to viral diseases or, being synthesized by plants have antiviral properties in animals. This reinforces the ubiquity of some essential molecules that are present in the different kingdoms and opens a new field of study. The presence of ABA, generally considered as the main phytohormone involved in abiotic stress responses, in many organisms including higher mammals (reviewed in Gómez-Cadenas et al., 2015) also supports this idea. Moreover, the obtained results also remark the use of LC-MS techniques to analyze the infection of CTV in citrus plants, which could be used in parallel with other emerging analytical alternatives (Killiny et al., 2017).

Funding

This work was supported by Ministerio de Economía y Competitividad (MINECO) and Universitat Jaume I through grants No. AGL2016-76574-R and UJI-B2016-23/UJI-B2016-24.

Conflict of interest statement

There is no conflict of interest for the co-authors.

Acknowledgements

Hormone measurements and metabolite profiling were carried out at the central facilities (Servei Central d'Instrumentació Científica, SCIC) of the Universitat Jaume I.

References

Alazem, M., Lin, N.S. 2015. Roles of plant hormones in the regulation of host-virus interactions. Mol. Plant Pathol. 16:529-540. https://doi.org/10.1111/mpp.12204.

Anderson, J.P., Badruzsaufari, E., Schenk, P.M., Manners, J.M., Desmond, O.J., Ehlert, C., Maclean, D.J., Ebert, P.R., Kazan, K. 2004. Antagonistic interaction between abscisic acid and jasmonate-ethylene signaling pathways modulates defense gene expression and disease resistance in Arabidopsis. Plant Cell 16:3460-3479. https://doi.org/10.1105/tpc.104.025833.

Arbona, V., Argamasilla, R., Gómez-Cadenas, A. 2010. Common and divergent physiological, hormonal and metabolic responses of *Arabidopsis thaliana* and *Thellungiella halophila* to water and salt stress. J. Plant Physiol. 167:1342-1350. http://dx.doi.org/10.1016/j.jplph.2010.05.012.

Arbona, V., Gómez-Cadenas, A. 2008. Hormonal modulation of Citrus responses to flooding. J. Plant Growth Regul. 27:241-250. http://dx.doi.org/10.1007/s00344-008-9051-x.

Argamasilla, R., Gómez-Cadenas, A., Arbona, V. 2013. Metabolic and regulatory responses in Citrus rootstocks in response to adverse environmental conditions. J. Plant Growth Regul. 33:169-180. http://dx.doi.org/10.1007/s00344-013-9359-z.

Baumert, A., Mock, H.P., Schmidt, J., Herbers, K., Sonnewald, U., Strack, D. 2001. Patterns of phenylpropanoids in non-inoculated and potato virus Y-inoculated leaves of transgenic tobacco plants expressing yeast-derived invertase. Phytochem., 56, 535–41. https://doi.org/10.1016/S0031-9422(00)00422-2

Ben Rejeb, K., Abdelly, C., Savouré, A. 2014. How reactive oxygen species and proline face stress together. Plant Physiol. Biochem. 80:278-284. https://doi.org/10.1016/j.plaphy.2014.04.007.

Bigeard, J., Colcombet, J., Hirt, H. 2015. Signaling mechanisms in pattern-triggered immunity (PTI). Mol. Plant 8:521-539. https://doi.org/10.1016/j.molp.2014.12.022.

Broekaert, W.F., Delauré, S.L., De Bolle, M.F.C, Cammue, B.P.A. 2006. The role of ethylene in host-pathogen interactions. Annu. Rev. Phytopathol. 44:393-416. https://doi.org/10.1146/annurev.phyto.44.070505.143440.

Cambra, M., Gorris, M.T., Román, M.P., Terrada, E., Garnsey, S.M., Camarasa, E., Olmos, A., Colomer, M. 2000. Routine detection of citrus tristeza virus by direct Immunoprinting-ELISA method using specific monoclonal and recombinant antibodies. Proceedings 14th International Conference of the Organization of Citrus Virologists (IOCV), Riverside, pp. 34-41.

Cheng, C., Zhang, Y., Zhong, Y., Yang, J., Yan S. 2016. Gene expression changes in leaves of *Citrus sinensis* (L.) Osbeck infected by *Citrus tristeza virus*. J. Hortic. Sci. Biotec. 91:466-475. https://doi.org/10.1080/14620316.2016.1173523.

Claussen, W. 2005. Proline as a measure of stress in tomato plants. Plant Sci. 168:241-48. https://doi.org/10.1016/j.plantsci.2004.07.039.

Culver, J.N., Padmanabhan. M.S. 2007. Virus-induced disease: altering host physiology one interaction at a time. Annu. Rev. Phytopathol. 45:221-243. https://doi.org/10.1146/annurev.phyto.45.062806.094422.

de Carvalho, K., de Campos, M.K.F., Domingues, D.S., Pereira, L.F.P., Vieira, L.G.E. 2013. The accumulation of endogenous proline induces changes in gene expression of several antioxidant enzymes in leaves of transgenic *Swingle citrumelo.* Mol. Biol. Rep. 40:3269-3279. https://doi.org/10.1007/s11033-012-2402-5.

Demkura, P.V., Ballaré, C.L. 2012. UVR8 Mediates UV-B-Induced Arabidopsis Defense Responses against Botrytis cinerea by Controlling Sinapate Accumulation. Mol. Plant 5, 1–11. https://doi.org/10.1093/mp/sss025.

Dória, M.S., de Sousa, A.O., Barbosa, C.J., Costa, M.G.C., Gesteira, A.S., Souza, R.M., Freitas, A.C.O., Pirovani, C.P. 2015. *Citrus tristeza virus* (CTV) Causing proteomic and enzymatic changes in sweet orange variety "Westin". PLoS ONE 10:e0130950. https://doi.org/10.1371/journal.pone.0130950.

Fu, S., Shao, J., Zhou, C., Hartung, J.S. 2017. Co-infection of sweet orange with severe and mild strains of Citrus tristeza virus is overwhelmingly dominated by the severe strain on both the transcriptional and biological levels. Front Plant Sci. 2017 Aug 31;8:1419. https://doi.org/10.3389/fpls.2017.01419.

Gandía, M., Conesa, A., Ancillo, G., Gadea, J., Forment, J., Pallás, V., Flores, R., Duran-Vila, N., Moreno, P., Guerri, J. 2007. Transcriptional response of *Citrus aurantifolia* to infection by *Citrus tristeza virus.* Virology 367(2):298-306. http://doi.org/10.1016/j.virol.2007.05.025

Glauser, G., Veyrat, N., Rochat, B., Wolfender, J.L., Turlings, T.C.J. 2013. Ultra-high pressure liquid chromatography-mass spectrometry for plants metabolomics: A systematic comparison of high-resolution quadrupole-time-of-flight and single stage Orbitrap mass spectrometers. J. Chromatogr. A 1292:151-159. https://doi.org/10.1016/j.chroma.2012.12.009.

Gómez-Cadenas, A., Vives, V., Zandalinas, S.I., Manzi, M., Sánchez-Pérez, A.M., Pérez-Clemente, R.M., Arbona, V. 2015. Abscisic Acid: A Versatile Phytohormone in Plant Signaling and Beyond. Curr. Prot. Pept. Sci. 16:413-434. https://doi.org/10.2174/1389203716666150330130102.

Hanssen, I.M., van Esse, H.P., Ballester, A.R., Hogewoning, S.W., Ortega Parra N., Paeleman, A., Lievens, B., Bovy, A.G., Thomma, B.P.H.J. 2011. Differential tomato transcriptomic responses induced by Pepino Mosaic Virus isolates with differential aggressiveness. Plant Physiol. 156:301-318. https://doi.org/10.1104/pp.111.173906.

Killiny, N., Hijaz, F., Harper, S.J., Dawson, W.O. 2017. Effects of *Citrus tristeza closterovirus* infection on phloem sap and released volatile organic compounds in *Citrus macrophylla*. Physiol. Mol. Plant Pathol. 98:25-36. https://doi.org/10.1016/j.pmpp.2017.03.003.

Kogovšek, P., Pompe-Novak, M., Petek, M., Fragner, L., Weckwerth, W., Gruden, K. 2015. Primary metabolism, phenylpropanoids and antioxidant pathways are regulated in potato as a response to *Potato virus Y* infection. PLoS ONE 11:e0146135. https://doi.org/10.1371/journal.pone.0146135.

López-Gresa, M.P., Lisón, P., Kim, H.K., Choi, Y.H., Verpoorte, R., Rodrigo, I., Conejero, V., Bellés, J.M. 2012. Metabolic fingerprinting of Tomato Mosaic Virus infected *Solanum lycopersicum*. J. Plant Physiol. 169:1586-1596. https://doi.org/10.1016/j.jplph.2012.05.021.

Matsuura, H.N., Rau, M.R., Fett-Neto, A.G. 2014. Oxidative stress and production of bioactive monoterpene indole alkaloids: Biotechnological implications. Biotechnol. Lett. 36:191-200. https://doi.org/10.1007/s10529-013-1348-6.

Moreno, P., Guerri, J., Ballester-Olmos, J.F., Albiach, R., Martínez, M.E. 1993. Separation and interference of strains from a Citrus Tristeza Virus isolate evidenced by biological activity and double stranded RNA (dsRNA) analysis. Plant Pathol. 42:35-41. https://doi.org/10.1111/j.1365-3059.1993.tb01469.x.

Moreno, P., Garnsey, S. M. 2010. *Citrus tristeza* diseases: a worlwide perspective, in: Karasev, A.V., Hilf, M.E (Eds) *Citrus tristeza virus Complex and Tristeza Diseases*. eds. The American Phytopathological Society, St Paul, MN, pp. 27–49.

Munshi, S.U., Taneja, S., Bhavesh, N.S., Shastri, J., Aggarwal, R., Jameel, S. 2011. Metabonomic analysis of hepatitis E patients shows deregulated metabolic cycles and abnormalities in amino acid metabolism. J. Viral Hepat. 18:e591–e602. https://doi.org/10.1111/j.1365-2893.2011.01488.x.

Pérez-Clemente, R.M., Montoliu, A., Vives, V., López-Climent, M.F., Gómez-Cadenas, A. 2015. Photosynthetic and antioxidant responses of Mexican lime (*Citrus aurantifolia*) plants to Citrus Tristeza Virus infection. Plant Pathol. 64:13-24. https://doi.org/10.1111/ppa.12241.

Radwan, D.E.M., Fayez, K.A., Mahmoud, S.Y., Hamad, A., Lu, G. 2007. Physiological and metabolic changes of *Cucurbita pepo* leaves in response to zucchini yellow mosaic virus (ZYMV) infection and salicylic acid treatments. Plant Physiol. Biochem. 45:480-489. https://doi.org/10.1016/j.plaphy.2007.03.002.

Santner, A., Calderon-Villalobos, L.I., Estelle M. 2009. Plant hormones are versatile chemical regulators of plant growth. Nat. Chem. Biol. 5:301-7. https://doi.org/10.1038/nchembio.165.

Spoel, S.H., Koornneef, A., Claessens, S.M.C., Korzelius, J.P., Van Pelt, J.A., Mueller, M.J., Buchala, A.J., Métraux, J.P., Brown, R., Kazan, K., Van Loon, L.C., Dong, X., Pieterse, C.M.J. 2003. NPR1 modulates cross-talk between salicylate- and jasmonate-dependent defense pathways through a novel function in the cytosol. Plant Cell 15:760-770. https://doi.org/10.1105/tpc.009159.

Ton, J., Flors, V., Mauch-Mani, B. 2009. The multifaceted role of ABA in disease resistance. Trends Plant Sci. 14:310-317. https://doi.org/10.1016/j.tplants.2009.03.006.

Vives-Peris, V., Gómez-Cadenas, A., Pérez-Clemente, R.M. 2017. Citrus plants exude proline and phytohormones under abiotic stress conditions. Plant Cell Rep. 36:1971-1984. https://doi.org/10.1007/s00299-017-2214-0.

Vlot, A., Dempsey, D A., Klessing, D.F. 2009. Salicylic acid, a multifaceted hormone to combat disease. Annu. Rev. Phytopathol. 47:177-206. https://doi.org/10.1146/annurev.phyto.050908.135202.

Yasuda, M., Ishikawa, A., Jikumaru, Y., Seki, M., Umezawa, T., Asami, T., Maruyama-Nakashita, A., Kudo, T., Shinozaki, K., Yoshida, S., Nakashita, H. 2008. Antagonistic interaction between systemic acquired resistance and the abscisic acid-mediated abiotic stress response in Arabidopsis. Plant Cell 20:1678-1692. https://doi.org/10.1105/tpc.107.054296.

Zahmanov, G., Alipieva, K., Denev, P., Todorov, D., Hinkov, A., Shishkov, S., Simova, S., Georgiev, M. I. 2015. Flavonoid glycosides profiling in dwarf elder fruits (*Sambucus ebulus* L.) and evaluation of their antioxidant and anti-herpes simplex activities. Ind. Crops Prod. 63:58-64. https://doi.org/10.1016/j.indcrop.2014.10.053.

Zandalinas, S.I., Rivero, R.M., Martínez, V., Gómez-Cadenas, A., Arbona, V. 2016. Tolerance of citrus plants to the combination of high temperatures and drought is associated to the increase in transpiration modulated by a reduction in abscisic acid levels. BMC Plant Biol. 16:105. https://doi.org/10.1186/s12870-016-0791-7.

Zhu, F., Xi, D.H., Yuan, S., Xu, F., Zhang, D.W., Lin, H.H. 2014. Salicylic acid and jasmonic acid are essential for systemic resistance against tobacco mosaic virus in *Nicotiana benthamiana*. Mol. Plant Microbe Interact. 27:567-577. https://doi.org/10.1094/MPMI-11-13-0349-R.

CAPTIONS

Figure 1. Proline content in *Citrus aurantifolia* sprouts. a: first year after infection b: second year after infection. Data are mean values of 3 independent determinations ± standard error. Different letters denote statistical differences, within each sprout age, at $p \leq 0.05$. (□) control plants, (▨) plants infected with mild isolate and (■) plants infected with severe isolate.

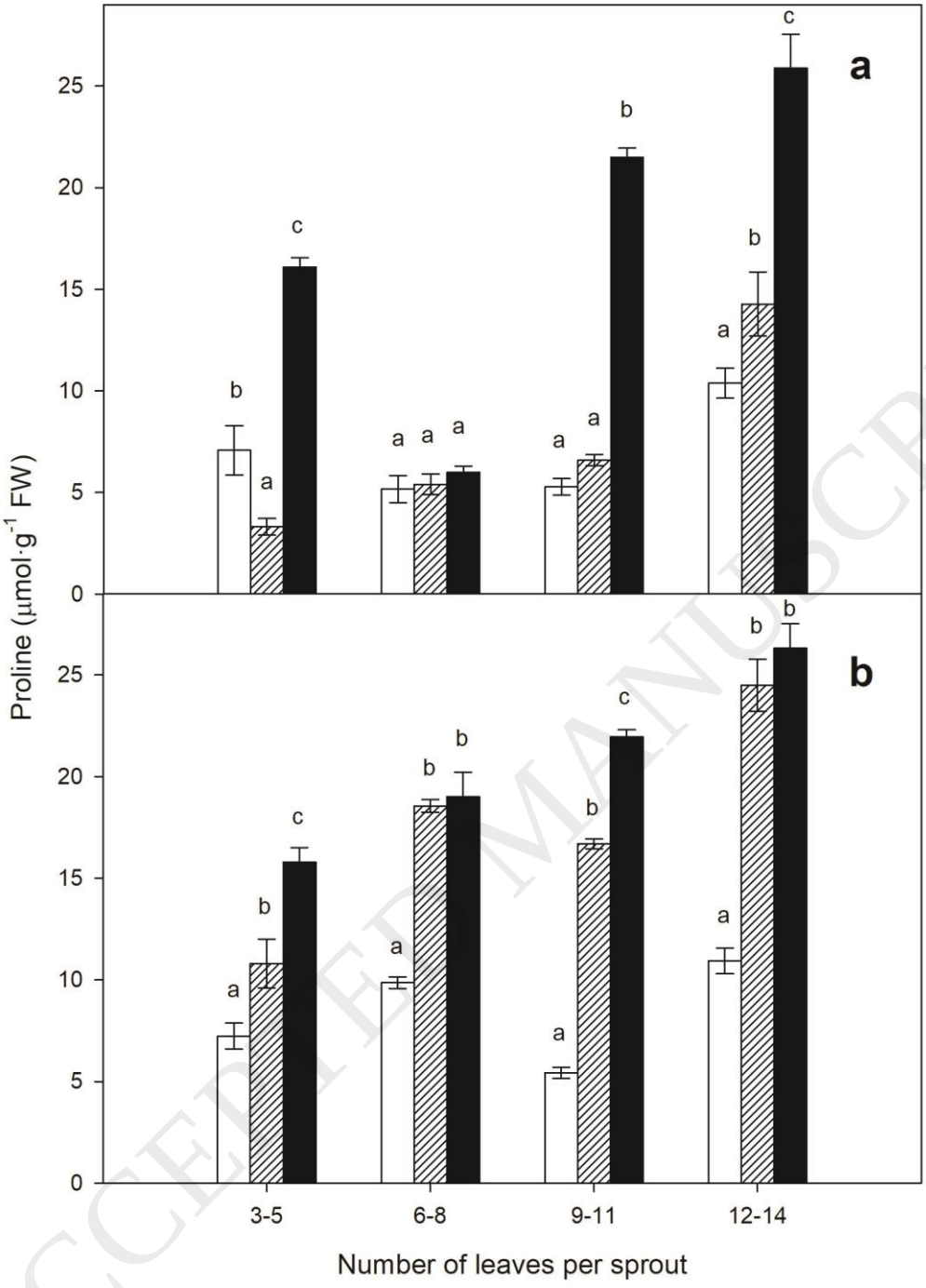

Figure 2. Abscisic acid content in *Citrus aurantifolia* sprouts. a: first year after infection b: second year after infection. Data are mean values of 3 independent determinations ± standard error. Different letters denote statistical differences, within each sprout age, at $p \leq 0.05$. (□) control plants, (▨) plants infected with mild isolate and (■) plants infected with severe isolate.

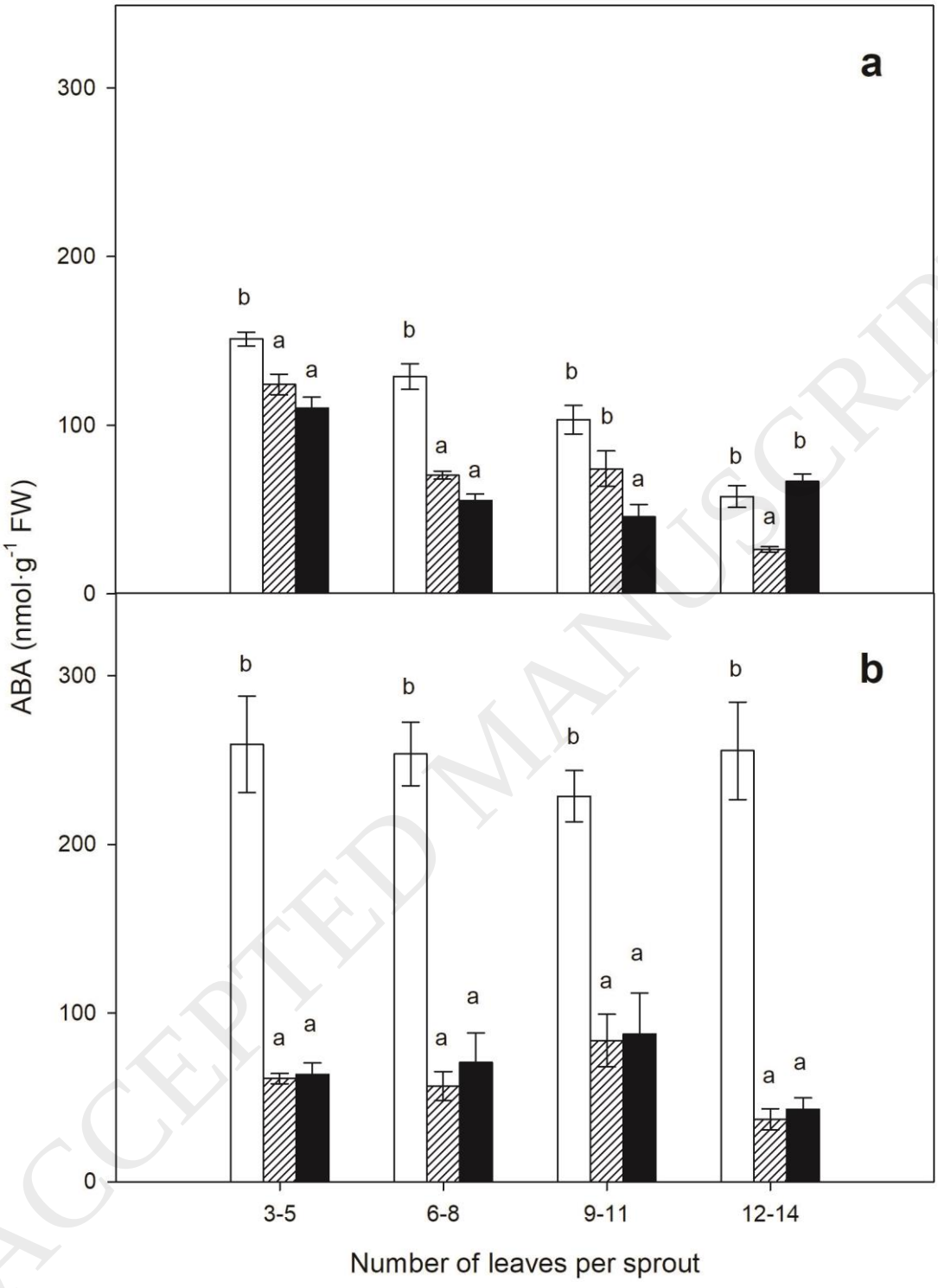

Figure 3. Salicylic acid content in *Citrus aurantifolia* sprouts. a: first year after infection b: second year after infection. Data are mean values of 3 independent determinations ± standard error. Different letters denote statistical differences, within each sprout age, at p

≤ 0.05. (□) control plants, (▨) plants infected with mild isolate and (■) plants infected with severe isolate.

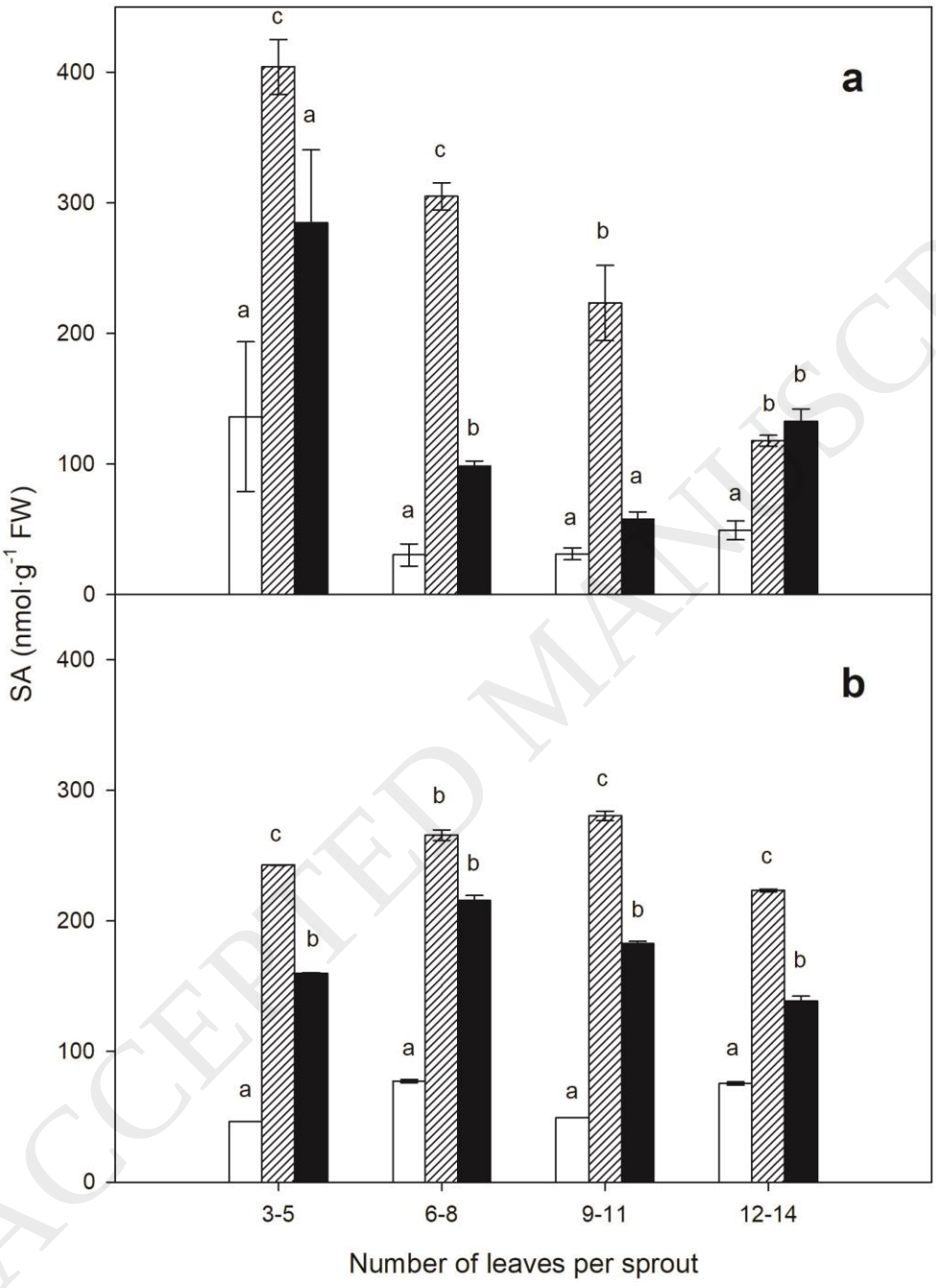

Figure 4. Jasmonic acid content in *Citrus aurantifolia* sprouts. a: first year after infection b: second year after infection. Data are mean values of 3 independent determinations ± standard error. Different letters denote statistical differences, within each sprout age, at p

≤ 0.05. (□) control plants, (▨) plants infected with mild isolate and (■) plants infected with severe isolate.

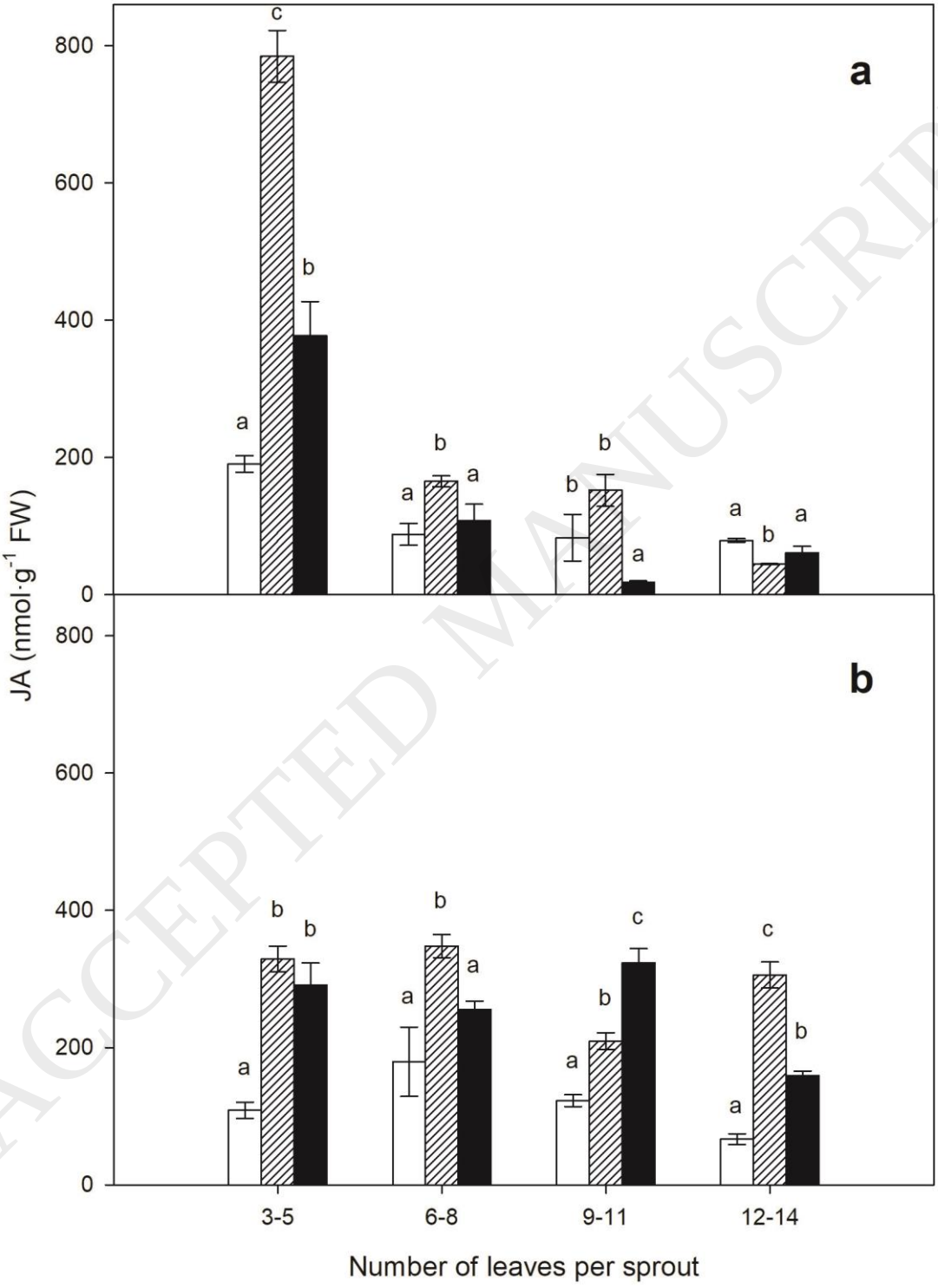

Figure 5. Partial Least Squares-Discriminant Analysis (PLS-DA) plot of secondary metabolite profiles in infected and uninfected samples of Mexican lime leaf sprouts.

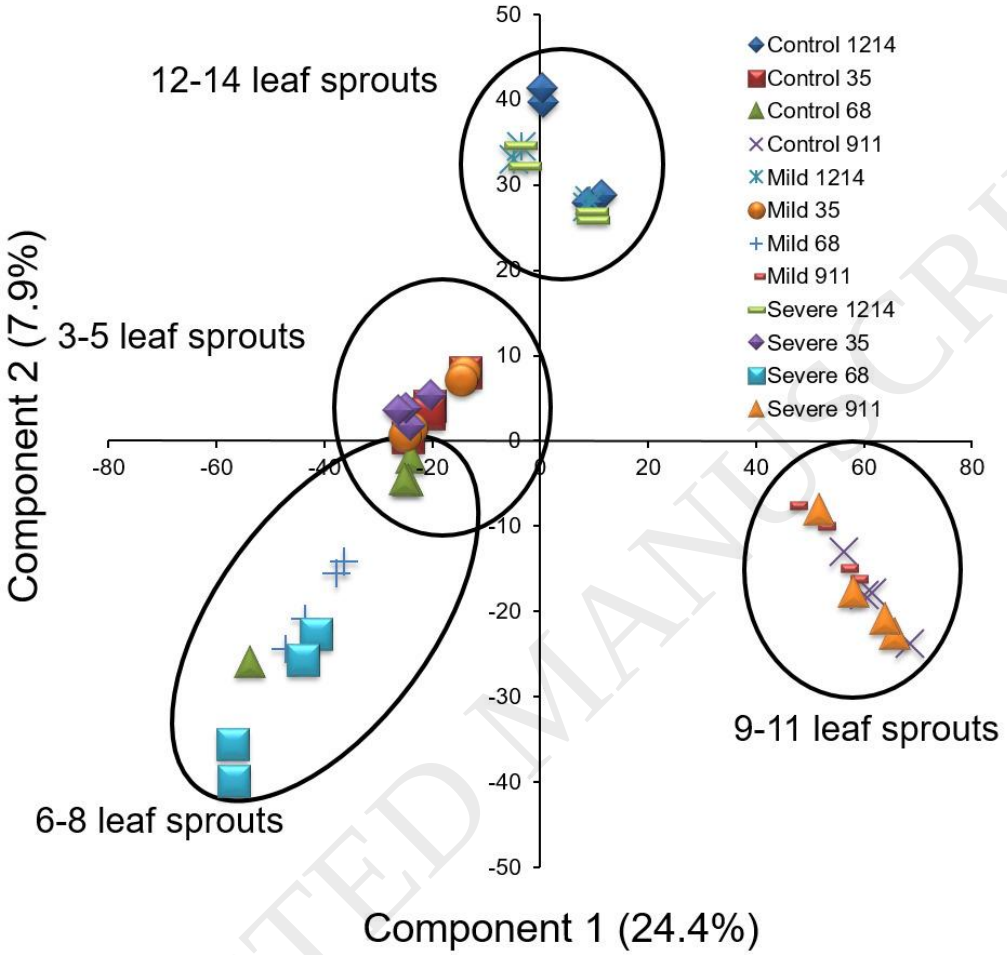

Figure 6. Metabolite profiling of control and CTV-infected *Citrus aurantifolia* sprouts**.**

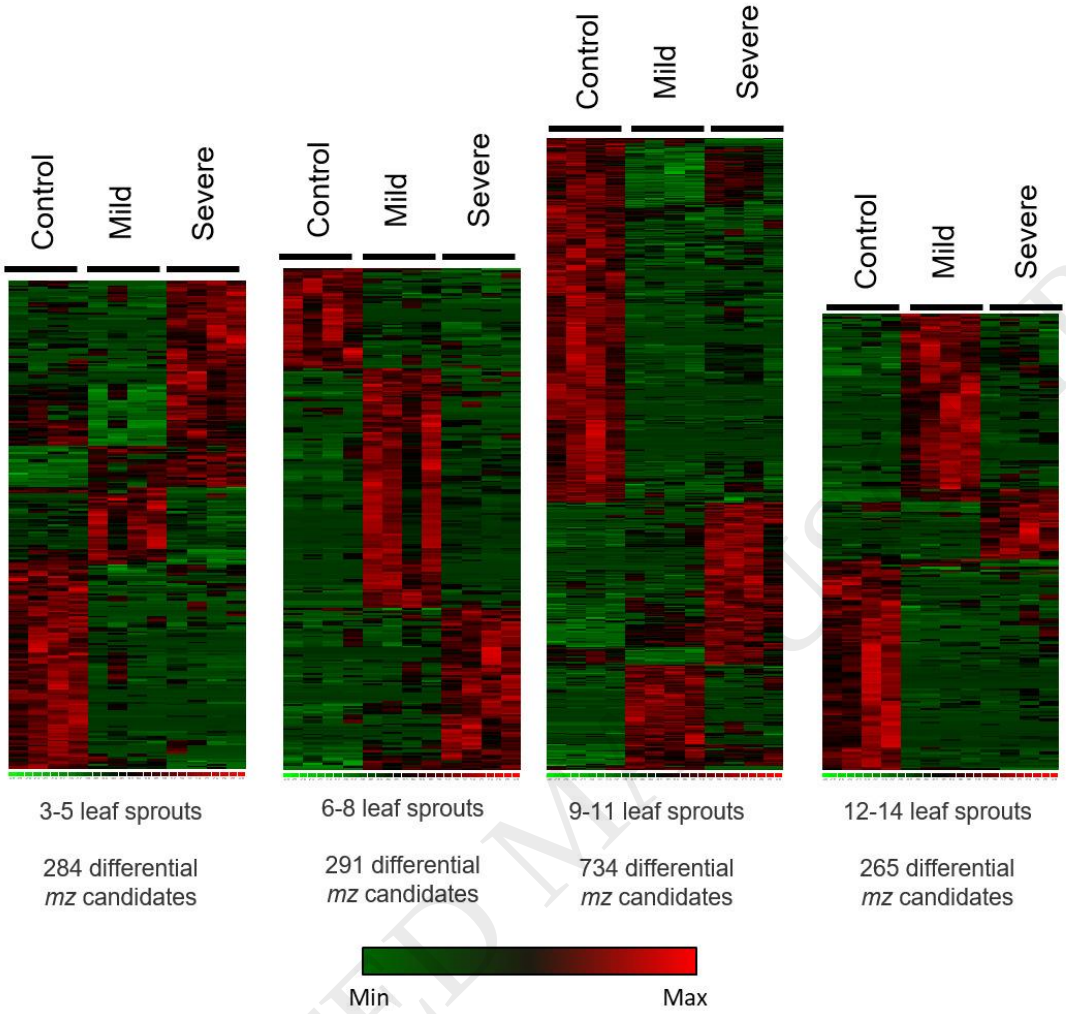

Figure 7. Hierarchical Cluster Analysis of differentially altered mass features ($p \leq 0.01$) in 3 to 5 leaf sprouts of *Citrus aurantifolia* control or CTV infected plants.

Figure 8. Hierarchical Cluster Analysis of differentially altered mass features ($p \leq 0.01$) in 6 to 8 leaf sprouts of *Citrus aurantifolia* control or CTV infected plants.

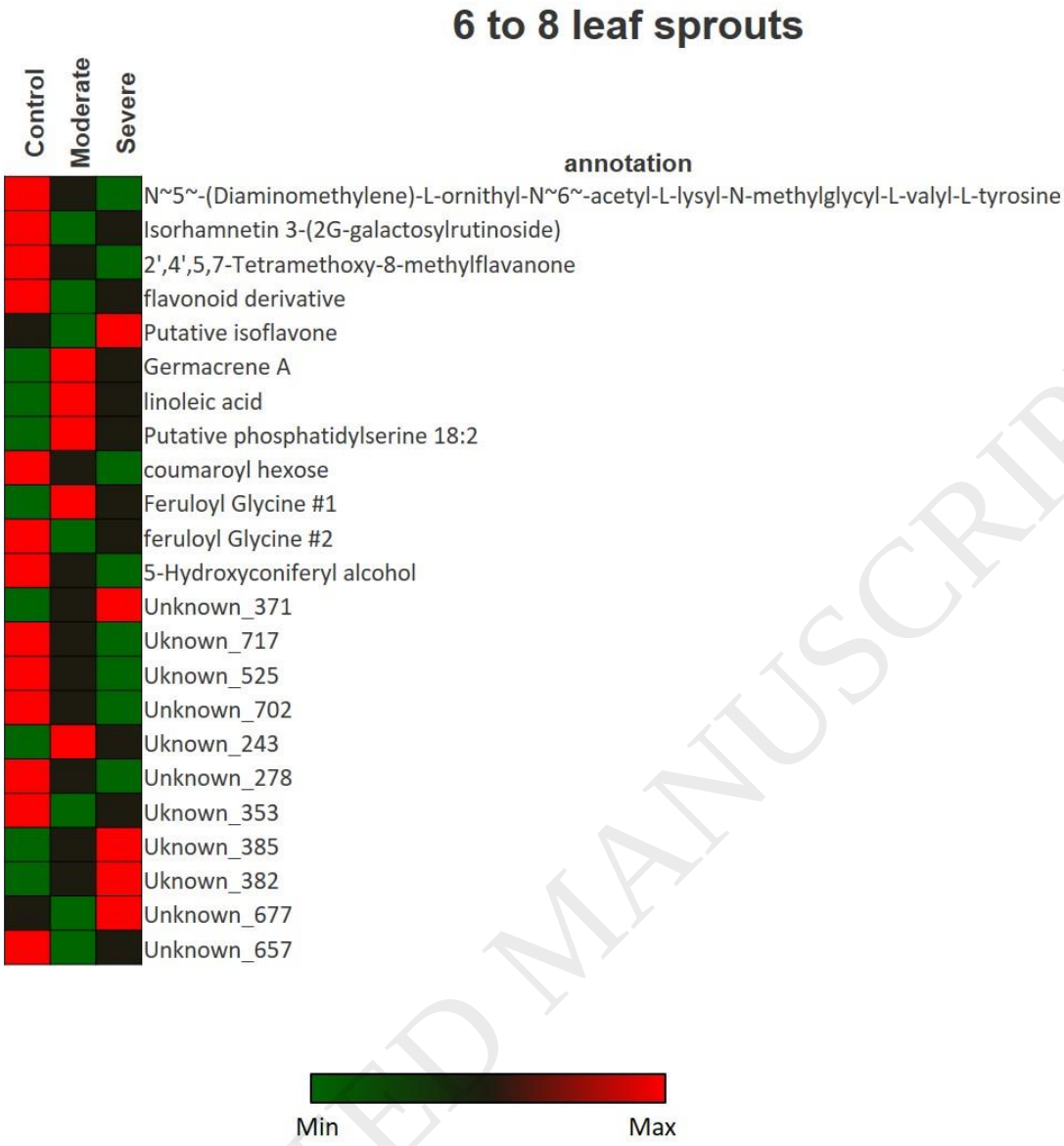

Figure 9. Hierarchical Cluster Analysis of differentially altered mass features ($p \leq 0.01$) in 9 to 11 leaf sprouts of *Citrus aurantifolia* control or CTV infected plants.

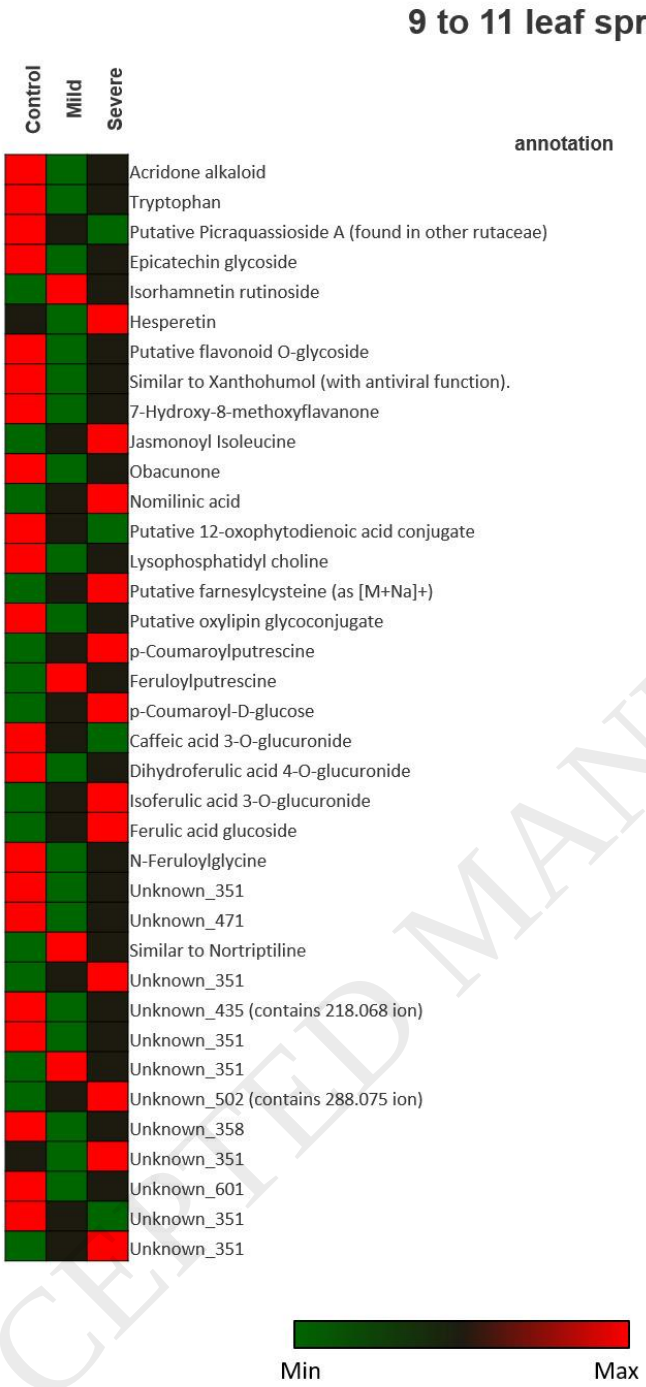

Figure 10 Hierarchical Cluster Analysis of differentially altered mass features ($p \leq 0.01$) in 12 to 14 leaf sprouts of *Citrus aurantifolia* control or CTV infected plants.